UNIVERSITÀ DEL PIEMONTE ORIENTALE

School of Medicine

Department of Health Sciences

Master's Degree in Medical Biotechnologies

Metabolomics in newly diagnosed diffuse large B-Cell lymphoma

Supervisor:

Dott. Riccardo MOIA

Firmato digitalmente da Riccardo Moia
Data: 27.09.2026 15:40:56 CEST
Organizzazione: UNIVERSITA' DEGLI STUDI DEL PIEMONTE ORIENTALE/01943490027

Candidate: Koggala Marakkalage Uthpala Kavindi Rupasinghe

Matricula number: 20063532

Academic Year 2025/2026

INDEX

ABSTRACT 3
1. INTRODUCTION 4
1.1. Diffuse large B-cell lymphoma 4
1.2. Cell of origin 5
1.3. Molecular pathogenesis of DLBCL 6
1.4. Genetic lesions associated with GCB-DLBCL 8
1.5. Genetic lesions associated with ABC-DLBCL 10
1.6. DLBCL sub-types and novel molecular clusters 11
1.7. DLBCL diagnosis, prognostic factors and treatment 14
1.8. Liquid biopsy applications in DLBCL 15
1.9. Metabolomics in DLBCL 17
2. AIM OF STUDY 20
3. MATERIALS AND METHODS 21
3.1. Patients included in the study 21
3.2. Separation of granulocytes from peripheral blood (PB) 21
3.3. Extraction of normal gDNA 21
3.4. Plasma ctDNA extraction 22
3.5. DNA quantification and fragmentation 22
3.6. Library design for hybrid selection 23
3.7. CAPP-seq library preparation 23
3.8. Metabolomic analysis 23
3.9. GCxGC/TOFMS analysis 24
3.10. Sample preparation for metabolomic analysis 25
3.11. Molecular characterization of the DLBCL cohort on ctDNA 25
3.12. Statistical Analysis 26
4. RESULTS 27
4.1. Characteristics of study participants 27
4.2. Association between metabolomic profile of the study cohort, cell of origin and molecular clusters 29
4.3. 2-hydroxubutyric acid (2HB) associates with poor outcomes in the study cohort 31
5. DISCUSSION 33
6. BIBLIOGRAPHY 35

ABSTRACT

Diffuse large B-cell lymphoma (DLBCL) is a biologically and clinically heterogeneous subtype of non-Hodgkin lymphoma. Approximately 60%-70% of patients achieve long-term disease control and are potentially cured with R-CHOP-based chemoimmunotherapy, whereas 30%-40% experience disease relapse or are refractory to treatment. Traditional prognostic tools, including the International Prognostic Index (IPI) and cell-of-origin (COO) classification, only partially capture the biological complexity underlying the heterogeneous clinical outcomes of patients with DLBCL. Therefore, the integration of complementary biomarkers is needed to improve risk stratification at diagnosis, including COO classification, molecular subgroups such as the DLBCL C1-C5 clusters, and circulating tumor DNA (ctDNA) levels. Moreover, the metabolomic profile may represent a novel host-related biomarker, although its potential prognostic and clinical relevance in DLBCL remains poorly investigated. Therefore, in the present study, we aimed to characterize the metabolomic profile of patients with DLBCL and to evaluate its potential clinical impact.

In this study, untargeted plasma metabolomics was performed in a cohort of 96 newly diagnosed patients with DLBCL treated with R-CHOP-based chemoimmunotherapy. A total of 280 plasma metabolites were identified. The metabolomic profile did not show differential associations with COO subtypes; however, several metabolic pathways showed nominal enrichment across the different molecular clusters identified by ctDNA analysis. Elastic-net Cox regression identified metabolites associated with progression-free survival (PFS), with 2-hydroxybutyric acid (2-HB) emerging as the only metabolite significantly associated with different PFS in the study cohort.

Plasma 2-HB represents a novel host-derived prognostic biomarker in newly diagnosed DLBCL and may, in the future, be integrated with established molecular and clinical biomarkers to further improve disease risk stratification.

1. INTRODUCTION

1.1. Diffuse large B-cell lymphoma

Diffuse large B- cell lymphoma (DLBCL) is the most common subtype of non-Hodgkin lymphoma (NHL), accounting for approximately 30-35% of all newly diagnosed cases worldwide (Dondolin *et al.*, 2025). DLBCL is most commonly diagnosed in people in their mid-60s, with about 30% of cases occurring in those over 75. No history of lymphoma has been detected in the majority of patients (Pasqualucci and Dalla-favera, 2018; Sehn and Salles, 2021). It is an aggressive disease, often marked by rapidly growing lymph nodes and systemic symptoms, requiring Immediate Medical Intervention.

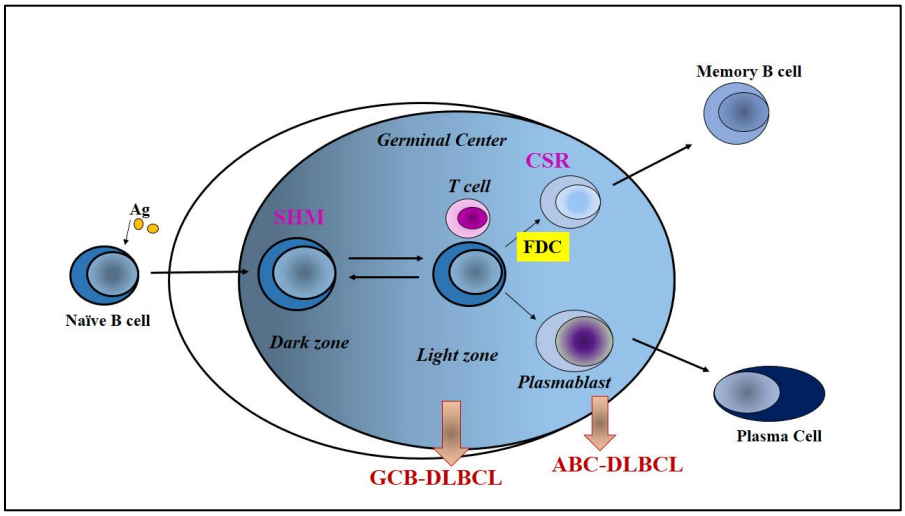


Figure 1- Cell of Origin of DLBCL subtypes .

DLBCL represents a biologically and clinically heterogeneous group of lymphoid neoplasms with diverse morphological, immune phenotypic, and clinical features (Chapuy *et al.*, 2018; Pasqualucci and Dalla-favera, 2018; Wright *et al.*, 2020; Wilson *et al.*, 2021).

DLBCL is defined by the diffuse proliferation of large neoplastic B cells, that exhibit vesicular nuclei, prominent nucleoli, and abundant cytoplasm, along with a high proliferative index. Immunophenotypic characterization demonstrates expression of pan-B-cell markers: CD19, CD20, CD22, and CD79a, which are essential for the diagnosis and form the basis for targeted immunotherapy (Rossi *et al.*, 2017).

The standard treatment is chemo immunotherapy (CI) with R-CHOP regimen (rituximab, cyclophosphamide, doxorubicin, vincristine, and prednisone), which leads to cure in approximately over 60% of patients (Pasqualucci *et al.*, 2011; Tilly *et al.*, 2015). More recently, the combination of polatuzumab vedotin with rituximab, cyclophospamide,

doxorubicin, and prednisone (Pola-R-CHP) has also emerged as a frontline standard, particularly in patients with intermediate- to high-risk DLBCL based on the international prognostic index (IPI) score (Tilly *et al.*, 2022).

However, the heterogeneity in the molecular landscape of DLBCL presents challenges in assessing response to treatment, prognosis, and the identification of patients with early relapsing/refractory disease after first-line chemo immunotherapy (Moia *et al.*, 2025).

1.2. Cell of origin

DLBCL occurs as a result of an expansion and progressive accumulation of mature and malignant B lymphocytes, at different stages of differentiation. During B lymphocyte ontogeny, after arising in the bone marrow (BM), these cells migrate to secondary lymphoid tissues, where they encounter their respective antigens that stimulate the development of secondary follicles. Within the germinal centers (GCs) of these follicles, B lymphocytes are involved in clonal expansion somatic hypermutation, and antibody affinity maturation processes that are essential for the production of high-affinity antibodies (Silva and Klein, 2015; Mesin, Ersching and Victora, 2016).

DLBCL results from the malignant transformation of mature B-cells that have experienced the GC reaction. GCs are dynamic compartments that form when B-cells are challenged by a foreign antigen and represent the primary site for clonal expansion and antibody affinity maturation (Silva and Klein, 2015; Mesin, Ersching and Victora, 2016). Dysregulation of these processes can disrupt normal B-cell maturation and promote lymphomagenesis.

Molecular diagnosis of Diffuse large B-cell lymphoma subtypes comes with the advent of gene expression profiling (GEP), which was used to define two prominent cell-of-origin (COO) subtypes in about 80%-85% of cases, *i)* germinal center B-cell like (GCB) DLBCL and *ii)* activated B-cell like (ABC) DLBCL, with unclassified cases (Alizadeh *et al.*, 2000; Basso and Dalla-favera, 2015; Chapuy, Stewart, Andrew J. Dunford, *et al.*, 2018)

These subtypes are characterized by distinct transcriptional programs, oncogenic signaling pathways, and clinical outcomes. The ABC-DLBCL subtype is associated with chronic active B-cell receptor signaling and constitutive activation of nuclear factor κB (*NF-κB*), conferring a poorer prognosis compared with the GCB-DLBCL subtype, which reflects gene expression patterns of normal germinal center B-cells (Liu and Barta, 2019). ABC-

DLBCL is generally associated with poorer responses to standard treatments compared with GCB-DLBCL (Thieblemont *et al.*, 2011; Dunleavy and Wilson, 2014; Scott *et al.*, 2015).

1.3. Molecular pathogenesis of DLBCL

The pathogenesis of DLBCL involves numerous genetic alterations. Some of these are shared between the two main molecular subtypes GCB-DLBCL and ABC-DLBCL, while others are subtype-specific. Common genetic abnormalities found in both GCB- and ABC-DLBCL include: i) alterations in histone/chromatin-modifying enzymes; ii) dysregulation of *BCL6* activity; iii) mechanisms enabling immune evasion; and iv) additional mutations, including somatic copy number alterations (SCNs) and structural variants (SVs).

1.3.1. Alterations of histone/chromatin modifiers

The most frequent genetic lesion in DLBCL can be explicited as somatic mutation of *KMT2D* gene which is known as lysine-specific methyltransferase 2D, detected in approximately 30% of cases (Morin *et al.*, 2011; Pasqualucci *et al.*, 2011). *KMT2D* is a *SET1* family histone methyltransferase that trimethylates *H3K4* to elevate active chromatin (Shilatifard, 2012).

Furthermore, over one third of DLBCL expresses somatic mutations and/or deletions affecting acetyltransferase gene coding for CREB binding protein (*CREBBP*) (more common with ~50% in GCB-DLBCL compared to ABC-DLBCL at ~30%) (Pasqualucci *et al.*, 2011).

However, DLBCL-associated mutations and small insertion or deletion which are known as indels disrupt and impair the function of *CREBBP/EP300* proteins either deleting the histone acetyltransferasr domain or by introducing amino acid alterations within this domain, which imply diminished affinity for Acetyl-coenzyme A (CoA) (Pasqualucci *et al.*, 2011).

1.3.2. Deregulation of BCL6 activity

Mutations of *BCL6*, a proto-oncogene were discovered in 61% of DLBCL events with a significantly higher prevalence in GCB-DLBCL (>70%) compared to ABC-DLBCL (~44%). The principle processes of molecular lesions of *BCL6* gene are translocation and somatic hypermutation (SHM). Chromosomal translocations substitute the *BCL6* promoter with heterologous sequences from variety of translocation partners, while SHM influences first intron of *BCL6* gene and, at a lower frequency, first non-coding exon. In addition to direct

gene influences, *BCL6* expression is indirectly deregulated by alternative mechanisms of genetic lesions, such as *CREBBP/E300* mutations that have deleterious effects, can impair acetylation-mediated *BCL6* inactivation (Bereshchenko, Gu and Dalla-favera, 2002; Pasqualucci *et al.*, 2011; Pasqualucci and Dalla-favera, 2018).

Nonetheless, the elevation of *BCL6* mutations has not been revealed to have disease progression (Iqbal *et al.*, 2007).

1.3.3. Escape from immune surveillance

As a result of genetic and epigenetic mechanisms, DLBCL commonly flops to express the regulation of cell surface molecules, such as major histocompatibility complex (MHC) class I, which is essential for the immune effector cells undergoing tumor cell recognition. Inactivating mutations and deletions within β2-microglobulin (*BM2*) locus are represented as mechanisms, while Preventing the coding of *BM2* protein, mandatory for the formation of cell surface expression of the human leukocyte antigen class I (*HLA-1*), involved in CD8+ cytotoxic T cells recognition (Challa-malladi *et al.*, 2011).

1.3.4. Alternative genetic lesions

DLBCL has undergone several other genetic lesions. *TP53* mutations are detectable in approximately 20% of DLBCL cases as an independent predictor of poorer prognosis as have been illustrated by studies. *TP53* genetic lesions are consistently retained as loss-of-function and can occur in the DNA binding domain, with a negative prognostic impact (Young *et al.*, 2007; Xu-monette *et al.*, 2012; Karube *et al.*, 2018). Forkhead box protein O1 (*FOXO1*) gene mutations were observed in 8.6% of DLBCL cases. 92.3% of these mutations were localized in the first exon, 46.2% were refractory mutations influencing N-terminal region while 38.5% have correlated with DNA binding domain, consist amino acid alterations, preventing *FOXO1* inactivation in response to phosphoinositide 3-kinase (*PI3K*) signaling, a transcription factor which is a principle role player during B-cell differentiation (Trinh *et al.*, 2013; Karube *et al.*, 2018). Furthermore, its activity is negatively regulated by *PI3K/AKT* signaling pathway (Dominguez-sola *et al.*, 2015).

However as a consequence, *FOXO1* genetic variations diminish overall survival (OS) in patients treated with R-CHOP (Trinh *et al.*, 2013).

1.4. Genetic lesions associated with GCB-DLBCL

In DLBCL, certain genetic abnormalities are more common with GCB-DLBCL. These include: i) chromosomal translocations involving the B-cell lymphoma/leukemia 2 (*BCL2*) and myelocytomatosis viral oncogene homolog (*MYC)* genes; ii) mutations of the enhancer of zeste homolog 2 (*EZH2*) methyltransferase gene; iii) mutations of the tumor necrosis factor-receptor superfamily member 14 (*TNFRSF14*) and iv) alterations affecting B-cell migration.

i. Chromosomal translocations of BCL2 and MYC

In most tissues, *BCL2* is detected as a main anti-apoptotic protein that prevents cell death. However, it is basically absent in GC due to the maintenance of a default pro-apoptotic mechanism by GC B-cells. The t(14;18) translocation juxtaposes the *BCL2* coding exons in approximately 30% of DLBCL cases under the control of immunoglobulin (IG) locus, impacting its constitutive expression. Additionally, an inferior outcome has evolved with dysregulation of *BCL2* via coupling with *MYC* deregulation (Barrans *et al.*, 2003). Moreover, MYC translocations are detected with a frequency range within 5% to 15% in DLBCL (Schiefer *et al.*, 2015). Several studies revealed that DLBCL lesions with simultaneous *BCL2* and *MYC* translocations which are known as double hit lymphomas (DHL) while additional *BCL6* gene break events which are known as triple hit lymphomas (THLs) (Schiefer *et al.*, 2015). Isolated *MYC* rearrangements have weaker prognostic relevance that is compared to *BCL2* isolated translocations (Visco *et al.*, 2012).

According to the World Health Organization (WHO) classification, High grade B-cell lymphoma (HGBL) was introduced as new phenomenon, defined by the presence of *MYC* and *BCL2* and/or *BCL6* rearrangements, poor prognosis, and DLBCL morphology when R-CHOP chemotherapy has been undergone (Martinez, 2017). Additionally, in most recent WHO classification, studies discovered the incorporate advances in molecular characterization which is defined to this category. HGBL with *MYC* and *BCL2* and/or *BCL6* rearrangements alone have been reclassified as either DLBCL, not otherwise specified (DLBCL-NOS) or HGBL, NOS (Alaggio *et al.*, 2022). High-grade morphology and aggressive clinical composition are characteristic to double hit (DH) lymphomas, with poor responsiveness to standard R-CHOP chemoimmunotherapy (Barrans *et al.*, 2010).

ii. Mutations of EZH2 methyltransferase

EZH2 encodes histone methyltransferase, which contains a SET-domain, responsible for trimethylation of the lysine 27 residue of histone H3 (*H3K27me3*) (Czermin *et al.*, 2002). Furthermore, in about 22% of GCB-DLBCL illustrate heterozygous *EZH2* gene mutations. In most cases, these mutations substitute a single evolutionary conserved tyrosine residue (Y641) within the protein SET domain, elevating its capability to catalyze the addition of *H3K27me3* spot (Morin *et al.*, 2010; Sneeringer *et al.*, 2010).

iii. Mutations in TNFRSF14

TNFRSF14 encodes for a member of the tumor necrotic factor-receptor superfamily that is expressed in both T and B-cells and can deliver opposing signals based on its specificity for diverse ligands (Steinberg, Cheung and Ware, 2011). Poor OS and progression-free survival (PFS) are retained as a consequence of high *TNFRSF14* expression (Carreras et al., 2019). Furthermore, deletions and mutations are included in *TNFRSF14*, ~50% as missense, ~40% as nonsense, and 2.5% as frame shift events confined to the exons encoding for its actodomain, are recurrently detected in DLBCL and segregate with GCB subtype as approximately 30% of cases (Boice *et al.*, 2016). The inhibition of cell-cell interactions between receptor and its ligand B- and T-lymphocyte attenuator (BTLA), which induces a tumor-supportive microenvironment, is illustrated as one mechanism revealing the tumorigenic effect of the loss of *TNFRSF14* (Boice *et al.*, 2016).

iv. Alterations in B-Cell Migration

The GC, specialized microstructure in secondary lymphoid tissues, physiologically produces antibody secreting plasma cells and memory B-cells to protect against recurrent infection (Stebegg *et al.*, 2018). The activity of two GC-specific-G-protein coupled receptors (*GPCRs*) which are known as sphingosine-1-phosphate receptor 2 (*S1PR2*) and the orphan purinergic receptor *P2RY8* modulate the confinement of B-cells within microenvironment (Green and Cyster, 2012). Furthermore, these two receptors recruit two closely related G proteins such as Ga12 and Ga13 to stimulate *RHOA* activity via specific guanine nucleotide exchange factors, suppressing *pAKT* signaling and cell migration in response to lipid ligands. Recurrent inactivation of the mutations in various of components in this pathway, including the *SIPR2, GNA13*, and rarely, *ARHGEF1* and *P2RY8* genes (overall, 30% of cases) is detected in GCB-DLBCL, but not in ABC-DLBCL (Cattoretti *et al.*, 2009; Muppidi *et al.*, 2014).

Moreover, in mouse models, deletion of these genes is correlated with disruption of the GC microstructure, followed by dissemination of GC B-cells to peripheral blood and bone marrow, eventually leading to lymphomagenesis that exhibit characteristics of GCB-DLBCL (Cattoretti *et al.*, 2009; Muppidi *et al.*, 2014).

1.5. Genetic lesions associated with ABC-DLBCL

The key biology of ABC-DLBCL is defined by alterations that result in the constant activation of the *NF-κB* pathway, which is essential for the survival of ABC-DLBCL cells (Pasqualucci *et al.*, 2011). These alterations include: i) mutations in the BCR signaling pathway; ii) mutations of myeloid differentiation primary response 88 (*MYD88*); iii) mutations of tumor necrosis factor alpha-induced protein 3 (*TNFAIP3*); and iv) lesions blocking terminal B-cell differentiation.

i) . Mutations in BCR signaling pathway

Genetic alterations affecting components of the *BCR* signaling cascade are among the most defining features of ABC-DLBCL. Mutations in *CD79A* and *CD79B* occur in approximately 20%-25% of cases, leading to impaired receptor internalization and enhanced surface *BCR* expression, thereby sustaining chronic signaling. Additionally, activating mutations in *CARD11* (~10%) enable downstream *NF-κB* activation of survival pathways and are present in over 2/3 of ABC-DLBCL tumors, highlighting their critical role in lymphomagenesis (Chapuy, Stewart, Andrew J. Dunford, *et al.*, 2018; Roland Schmitz *et al.*, 2018; Sha *et al.*, 2019).

ii) . *Mutations in MYD88*

Among the most characteristic genetic lesions in ABC-DLBCL are mutations in *MYD88*, particularly the L265P variant, which is detected in approximately 25%-35% of cases. This mutation promotes spontaneous assembly of the myddosome complex, leading to activation of *NF-κB* and *JAK-STAT* signaling pathways independent of upstream receptor engagement. Furthermore, *MYD88* mutations frequently co-occur with *CD79B* mutations (~15%-20% of patients), defining the MCD subtype, which is associated with extranodal disease and adverse prognosis. These findings underscore the central role of innate immune signaling dysregulation in ABC-DLBCL pathogenesis (Bojarczuk *et al.*, 2019; Lacy *et al.*, 2020; Visco *et al.*, 2020; Wright *et al.*, 2020a).

iii). Aberrations of TNFAIP3

Biallelic muations and/or focal deletions has been shown by about 30% of ABC-DLBCL lesion events while inactivating the tumor necrotic factor alpha-induced protein 3 (*TNFAIP3*) gene, which encodes a dual-function ubiquitin-editing enzyme involved in negatively regulating *NF-κB* responses triggered by *TLR* and *BCR* signaling (Boone *et al.*, 2004; Compagno *et al.*, 2009; Kato *et al.*, 2009). The loss of *TNFAIP3/A20* function may contribute to lymphomagenesis by allowing *NF-κB* responses to persist inappropriately for extended periods (Compagno *et al.*, 2009; Kato *et al.*, 2009).

iv) . Lesions blocking terminal B-cell differentiation

In ABC-DLBCL, the genetic-driven, intrinsic activation of *NF-κB* is often concomitantly driven by the alterations that block terminal B-cell differentiation (Pasqualucci and Dalla-favera, 2018). In particular, 25% of cases exhibit biallelic loss-of-function mutations or deletions in the PR domain-containing protein 1 (*PRDM1*)/ β-interferon gene positive regulatory domain I-binding factor (*BLIMP1*), a transcriptional repressor crucial for the B-cell plasmacytic differentiation and vital for plasma cell (PC) development (Pasqualucci *et al.*, 2006).

1.6. DLBCL sub-types and novel molecular clusters

Classification of DLBCL into subgroups has been undergone by GEP based on COO, ABC, GCB, and unclassified, each of which is correlated with different responses to chemotherapy and targeted therapies (Alizadeh *et al.*, 2000; Rosenwald and Wright, 2002). Although this classification accounted for some of the heterogeneity in the clinical outcome following R-CHOP chemotherapy, it does not fully account for the diverse responses and outcomes observed with R-CHOP or targeted treatments. The extreme genetic and phenotypic heterogeneity of DLBCL continues to reveal challenges to the development of precision therapies (Wright *et al.*, 2020a).

To account for this complexity, variety of mathematical-based clustering methods have been utilized to stratify DLBCL tumors into genetic subtypes that are characterized by genomic aberrations in subtype specific hallmark genes. Identification of genes which are recurrently altered by mutations, translocations, and copy number variations (CNVs) has been enabled by integrating genomic data from multiple analytical methods (Chapuy, Stewart, Andrew J Dunford, Kim, Kamburov, Staiger, *et al.*, 2018; Roland Schmitz *et al.*, 2018).

Clinical significance of these genetic subtypes was evolved by their association with outcomes along with R-CHOP therapy (Wright *et al.*, 2020a).

In 2018, Chapuy and colleagues performed whole-exome sequencing (WES) with an expanded bait set to capture known structural changes SVs in 304 newly diagnosed DLBCL events. Five distinct molecular clusters (C1-C5) were identified along with and additional subset without detectable alterations (C0) (Chapuy, Stewart, Andrew J Dunford, Kim, Kamburov, Staiger, *et al.*, 2018).

Cluster 5: Most frequently, *BCL2* gain-of-function alterations, mutations in $MYD88^{L265P}$, and *CD79B* were illustrated (Chapuy, Stewart, Andrew J. Dunford, *et al.*, 2018).

Cluster 1: Key genetic lesions of this cluster are *BCL6* SVs and mutations of the *NOTCH2* signaling pathway, concurrent with multiple genetic bases of immune escape, and inactivating mutations. The majority of C1 and C5 DLBCLs were classified as ABC-type tumors by transcriptional profiling, suggesting different targeted treatment strategies in genetically different ABC-DLBCLs: inhibition of *BCR/TLR* signaling and *BCL2* in C5 and lesion of *NOTCH* and *BCL6* signaling and immune evasion mechanisms in C1 (Chapuy, Stewart, Andrew J. Dunford, *et al.*, 2018).

Cluster 3: *BCL2* aberrations, frequent mutations in chromatin modifiers, *KMT2D, CREBBP, EZH2,* and *PTEN* inhibiting mutations are illustrated as the key components of cluster 3 signature (Chapuy, Stewart, Andrew J Dunford, Kim, Kamburov, Staiger, *et al.*, 2018).

Cluster 4: Mutations in frequent immune evasion molecules (*CD83*), intermediates of *BCR/PI3K (SGK1), RAS/JAK/STAT* pathway members, and *NF-κB* modifiers (*CARD11*) were detected in this cluster type. Genetically distinct GCB tumor subsets were revealed by C4 and C3 clusters, with potential therapies targeting *BCL2, PI3K*. Moreover, epigenetic modifications were integrated in C3 GCB tumors including *EZH2* and *CREBBP*, and modifiers in C4 GCB tumors including *JAK/STAT* and *BRAF/MEK1* blockade (Chapuy, Stewart, Andrew J Dunford, Kim, Kamburov, Staiger, *et al.*, 2018).

Cluster 2: This cluster is defined mostly by biallelic inactivation of *TP53* through lesions, mutations and 17p copy loss and is demonstraed both in GCB and ABC-DLBCL subtypes (Chapuy, Stewart, Andrew J Dunford, Kim, Kamburov, Staiger, *et al.*, 2018).

Cluster 0: This cluster has been determined as a small subset of DLBCLs while lacking genetic drivers (Chapuy, Stewart, Andrew J Dunford, Kim, Kamburov, Staiger, *et al.*, 2018).

Nonetheless, in this study, prognostic significance of the newly specified coordinate genetic signatures was assessed and significant distinctions in PFS and OS were identified. The patients allocated to C0, C1, and C4 DLBCL subtypes had more beneficial outcomes compared to those pertaining to C3 and C5 gene clusters (Chapuy, Stewart, Andrew J Dunford, Kim, Kamburov, Staiger, *et al.*, 2018).

In 2018, approximately 500 DLBCL events were examined by Schmitz and his colleagues by utilizing exome and transcriptome sequencing, array-based DNA CN analysis, and targeted resequencing of 372 genes to detect more refractorical aberrant genes and signaling pathways (R Schmitz *et al.*, 2018). Moreover, four genetic DLBCL subtypes were examined and detected by applying the predictor algorithm Geneclass including **MCD** was detected based on the co-occurrence of $MYD88^{L265P}$ and *CD79B* mutations, **BN2** was detected based on *BCL6* fusions and *NOTCH2* mutations, **N1** was detected based on *NOTCH1* mutations, and **EZB** was detected based on *BCL2* translocations and *EZH2* mutations. In addition, these subtypes are distinct with each other on the basis of gene expression signatures and responses to immunotherapy. Furthermore, an optimal survival was perceived in the BN2 and EZB subtypes, while substandard outcomes were detected in both MCD and N1 subtypes (R Schmitz *et al.*, 2018).

According to these certain observations, the genetic profiles were fused by Wright and his team in 2020 with these two studies to develop the LymphGen algorithm while providing a probabilistic differentiation equipment for DLBCL malignancy from an individual patient into a genetic subtype (Wright *et al.*, 2020a). They outlined a genetic subtype as a group of tumors that is enriched for genetic aberrations in a set of subtype predictor genes. These subtype predictor genes are demonstrated by concerning each possible combination of genetic lesions. LymphGen utilizes the presence or absence of each subtype predictor feature to provide a probability that a tumor belongs to the subtype (Wright *et al.*, 2020a).

To demonstrate the genetic costitution of the subtypes, a set of genetic features were selected and significantly associated with a subtype ($p \leq 0.01$) and were present >10% of the subtype. Initially, they close seeds representing the four previously examined genetic subtypes that are **MCD** including $MYD88^{L265P}$ and *CD79B* mutations, **BN2** including *BCL6* translocations and *NOTCH2* mutations, **N1** including *NOTCH1* mutations, and **EZB** including *EZH2* mutations and *BCL2* translocations. Hence, they evolved a seed class of cases with *TP53* features which is defined as "*A53*". Additionally, a second new seed class was generated based on the features of *SGK1* and *TET2* genes, termed "ST2" (Wright *et al.*, 2020a). This classification splits DLBCLs into seven genetic subtypes that distinct in

oncogenic pathway activation, gene expression phenotype, tumor microenvironment, survival, and potential therapeutic targets (Wright *et al.*, 2020a).

Latest breakthroughs in the molecular classification of DLBCL have resulted to the development of DLBclass, a next-generation probabilistic classifier configured to promisingly identify the five genetically known clusters (C1-C5). DLBclass integrates mutations/aberrations, SCNs, and SVs, while illustrating that extra parameters such as COO status (tumor ploidy), reflecting that natural enrichment of ABC tumors in C1 and C5 and GCB tumors in C3 and C4, while C2 residues COO-independent. Significantly, additional cluster-specific variations were clarified by the model, including new mechanisms of *NOTCH2/NF-κB* activation in C1, fortification of *MYC/BCL2* double translocations in C3, and C4 phenotype overlapping with T-cell/histiocyte-rich LBCL (Chapuy *et al.*, 2025).

DLBclass obtains a larger fraction of DLBCL cases that is compared to LymphGen and provides more actionable genetic information, offering a practical and comprehensive infrastructure for personalized treatment approaches (Chapuy *et al.*, 2025).

1.7. DLBCL diagnosis, prognostic factors and treatment

The excisional biopsy of a suspicious lymph node (LN) is used for specific diagnosis of DLBCL while revealing large clusters of cells that degrade the structural integrity of the follicle center and analyze positive for pan B-cell markers including *CD20* and *CD79A*. Additionally, utilizing immunohistochemical (IHC) stains or GEP is more beneficial to determine the COO aspect (Liu and Barta, 2019).

R-CHOP chemoimmunotherapy is the standard treatment for DLBCL patients. Rituximab, an antibody is included in this specific therapy which targets CD20 protein primarily existed on the surface of B-cells and many lymphoma cells accompanying with chemotherapy medications such as cyclophosphamide, doxorubicin, vincristin, and prednisone (Kwak, 2012; Chiappella *et al.*, 2013). As a result of this regimen, approximately 60-70% patients with DLBCL are cured of disease. Nevertheless, nearly 30-40% of patients will relapse or, in a small patient's subset, be refractory to R-CHOP treatment (Edeiros, 2018). R-CHOP therapy frustrations are predominantly owing to primary refractoriness or relapses following an initial complete response (CR) (Lyon-sud and Lyon, 2016).

Current advancement in frontline treatment for DLBCL is the utilization of polatuzumab vedotine, an antibody-drug conjugate in combination with rituximab, cyclophosphamide, doxorubicin, and prednisone (Pola-R-CHP). This treatment regimen has appeared as a novel

standard of care, especially for the patients with intermediate-to high-risk disease according to the International Prognostic Index (IPI) score (Tilly, 2022).

Furthermore, the distinct genetic subtypes of DLBCL can impact therapy decisions. As an example, the lesions influencing the BCR-dependent NF-κB are usual in the BN2, MCD, and A53 subtypes, suggesting that these may be excitable to Bruton tyrosine kinase inhibitors (BTKis). In fact, *MYD88^{L265P}* and *CD79B* mutations that are consisted as MCD-like tumors have represented a high sensitive rate (≥80%) to ibrutinib in relapsed events (Wilson *et al.*, 2015; Grommes *et al.*, 2017; Lionakis *et al.*, 2017). Moreover, MCD model was relied on IL-10 receptor signaling to activate *JAK1* and *STAT3* (Rui *et al.*, 2016), and a selective *JAK* inhibitor, which is defined as *INCB040093*, has illustrated the activity in fusion with a PI3Kδ inhibitor in non-GCB DLBCL cases (Phillips *et al.*, 2018). An *EZH2* mutation is carried in EZB model to respond specifically to *EZH2* inhibitors (Wright *et al.*, 2020a). Additionally, MCD, BN2, and EZB models are composed of *BCL2* variations, suggesting that therapies such as venatoclax or navitoclax may anticipate beneficial effect for these genetic subtypes (Mathews *et al.*, 2014).

GEP has anticipated new perceptions into DLBCL biology and led to the proceeding of IHC algorithm in routine clinical practice. Fluorescence in situ hybridization (FISH) is utilized to detect and identify the DHLs and this identification of DHLs is characterized by translocations involving *MYC* and *BCL2* or *BCL6,* is crucial as a result of the poor prognosis concurrent with R-CHOP. DHLs or THLs are associated with rearrangements of *MYC* with *BCL2* and *BCL6*, are correlated with a highly aggressive clinical course, poor response to conventional therapies, high relapse rates (Rosenthal *et al.*, 2017).

1.8. Liquid biopsy applications in DLBCL

Traditional diagnostic methods, such as tissue biopsy, often fail to fully capture the complexity of tumor heterogeneity across different anatomical compartments since it typically samples a single tumor site (Rossi et al., 2017). Nevertheless, tissue biopsy is an invasive technique with certain challenges for obtaining serial samples, which are crucial for real-time disease monitoring and therapeutic assessment (Talotta, Almasri and Cosentino, 2023). The limitations underline the necessity to discover new aspects for personalizing treatment and enhancing patient outcomes (Rossi *et al.*, 2017).

Liquid biopsy refers to the analysis and a diagnostic procedure of tumor-derived DNA molecules in the body fluids (urine, cerebrospinal fluid (CSF)) or in the blood serum,

particularly circulating tumor DNA (ctDNA), cell-free DNA (cfDNA), circulating lymphoma cells, extracellular vesicles, and other soluble biomarkers obtained from plasma, serum, CSF (Moia *et al.*, 2019; He *et al.*, 2026). Furthermore, liquid biopsy is a minimal intrusive methodology enables the identification of disease-related biomarkers across accessible methods (blood drawing or the collection of body fluids like saliva, CSF, urine, and stool) while this technique is highly advantageous compared to the conventional tissue biopsy due to its ability to capture tumor heterogeneity at multiple sites, assist real-time disease monitoring, and provide the permission for longitudinal sampling through treatment (Heitzer, Roberts and Speicher, 2019; Liu and Barta, 2019). cfDNA are cast into the blood stream by the apoptotic cells (Diaz and Bardelli, 2014). ctDNA has been referred as fragments of DNA liberated by tumor cells into the blood.

ctDNA has been referred as fragments of DNA liberated by tumor cells into the blood. ctDNA has emerged as the most clinically relevant and advantageous DNA molecule in DLBCL because it reflects tumor-specific somatic mutations, clonal architecture, and disease burden (Almasri *et al.*, 2025).

The limitations in accessing fresh tumor material from DLBCL tissue biopsies has avoided the rapid translation of DLBCL gene mutations into prognostic or predictive tools for the clinical proceeding (Rossi *et al.*, 2017). Hence, various kinds of sources of tumor DNA along with the support to complement the molecular diagnostic analyses that are obtained of formalin-fixed paraffin-embedded (FFPE) tissue biopsies (Rossi *et al.*, 2017).

In DLBCL, the use of ctDNA is a powerful tool for the detection of genetic alterations that otherwise might be missed in the tissue biopsy. Advanced sequencing technologies, such as cancer personalized profiling by deep sequencing (CAPP-seq), have demonstrated that ctDNA can detect hallmark genetic alterations associated with DLBCL subtypes, including mutations of *MYD88*, *CD79B*, and *EZH2*, making it a useful tool for disease genotyping, enabling molecular classification of DLBCL and guiding targeted therapies. Studies have shown a high concordance between ctDNA genotyping and tissue biopsy for detecting genetic alterations in DLBCL (rossi et al., 2017; Scherer et al., 2016; Spina et al., 2018).

The molecular classification of DLBCL was established mainly on the tissue biopsy, enabling the identification of clinically relevant genetic subtypes with distinct features (Chapuy et al., 2018; Wright et al., 2020). Recent evidence shows that LymphGen can also be applied reliably and effectively on ctDNA. Moia et al. has reported a 95.8% concordance rate in molecular cluster assignment between ctDNA and tissue biopsy, highlighting the reproducibility of molecular clustering on plasma (Moia et al., 2025). As with the tissue

biopsy studies, patients assigned to the A53 and MCD clusters exhibited poorer outcomes, while those in the ST2 and BN2 clusters showed significantly better outcomes (Moia et al., 2025).

In DLBCL, ctDNA has been quantified or used to track the tumor clonotypic immunoglobulin gene reaarangement for minimal residual disease monitoring (Kurtz et al., 2015; Roschewski et al., 2014).

Pretreatment ctDNA levels have been identified as a key prognostic biomarkers in DLBCL. Several studies have linked higher baseline ctDNA levels to poorer PFS and OS (Alig et al., 2021; Meriranta et al., 2022). Moreover, baseline ctDNA levels could also be integrated with molecular clusters identified on the liquid biopsy, this combined approach of integrating multiple ctDNA-derived biomarkers enhances the prognostic accuracy and allows for more precise risk stratification of DLBCL patients (Moia et al., 2025).

In addition to pretreatment prognostic value, the dynamic changes in ctDNA levels during therapy have been shown to reflect treatment response in DLBCL (Lauer et al., 2022). These molecular response biomarkers offer an additional tool for monitoring treatment response and may integrate traditional methods such as PET/CT scans (Roschewski et al., 2023).

Despite its potential, there are challenges to the widespread clinical adoption of liquid biopsy in DLBCL. These include the need for standardization in sample collection, processing, and analysis, as well as technical limitations in detecting low frequency mutations and tumor chromosomal translocations. These notions suggest that liquid biopsy is not a substitute for the tumor biopsy but instead provides complementary information in DLBCL (Rossi et al., 2017). Nevertheless, with ongoing technological progress, ctDNA analysis may be expected to become a part of routine clinical practice in DLBCL, enhancing personalized treatment and improving patient outcomes (Almasri et al., 2025).

1.9. Metabolomics in DLBCL

Metabolites are small molecules that arise as intermediate or end products of cellular metabolism and reflect the functional output of gene expression, protein activity and environmental influences. As downstream readouts of biological processes, they provide an integrative snapshot of the physiological state of an organism. The circulating metabolome captures not only tumor-associated alterations but also systemic host factors including immune activity, organ function and the microbiome (Schmidt *et al.*, 2021). Because of this

integrative nature, metabolomics has emerged as a promising approach for the discovery of novel prognostic biomarkers across various malignancies, including lymphomas (Mi *et al.*, 2021; Fei *et al.*, 2022; Montagne *et al.*, 2026).

In DLBCL, the integration of metabolomic profiling with established tumor-derived biomarkers may add a systemic biological dimension and enable a more comprehensive and granular risk stratification of the disease. ctDNA is a minimally invasive biomarker with established prognostic value in DLBCL, providing a dynamic measure of tumor burden and molecular disease the same blood features (Rossi *et al.*, 2017; Kurtz *et al.*, 2018). Combining ctDNA levels measurement and metabolomics-based biomarkers within sample might offer an integrated view of both tumor and host-related features, potentially refining risk assessment.

Furthermore, metabolomics refers to the systematic study of metabolites derived from small molecules in bio fluids and tissues and emerged as minimally invasive complement to genomic and transcriptomic profiling, since this has been applied directly to plasma, serum, and urine without the necessity of tumor tissue biopsy (Suman *et al.*, 2025; Montagne *et al.*, 2026). Recent studies has revealed that metabolomics studies are divided into targeted approaches, which quantify predefined metabolites based on a specific biological hypothesis, and untargeted approaches to target comprehensive approach due to possibility of some metabolites without prior assumptions (Suman *et al.*, 2025).

Furthermore, in 2025, gas chromatography-mass spectrometry (GC-MS), liquid chromatography-mass spectrometry (LC-MS), and nuclear magnetic resonance (NMR) spectroscopy have been used as the principle analytical approaches. GC-MS provides high responsiveness and reproducibility for small, volatile, polar compounds such as amino acids, sugars, and short-chain organic acids while requiring derivatization procedures. LC-MS is frequently referred to a broader range of polar and non-polar huge molecular weight molecules such as complex lipids and other metabolites which generate energy while involving in suppression of iron and the reproducibility is lower than GC-MS (Suman *et al.*, 2025). Moreover, the sensitivity is less in NMR compared to both GC-MS and LC-MS and a minimal sample proceeding is required by NMR technique, a non-destructive, highly reproducible, and illustrate informative structural configuration on lipoproteins, nucleotides, and other bioactive molecules (Suman *et al.*, 2025; Montagne *et al.*, 2026).

Moreover, In this context, an untargeted, high resolution plasma metabolomics strategy with subsequent metabolite verification may represent a valuable approach for identifying

candidate metabolic biomarkers and to provide insights into patient's systemic metabolomic condition.

2. AIM OF STUDY

The aims of the present study are:

i) to dissect the plasma metabolomic profile in newly diagnosed DLBCL;

ii) to evaluate the potential prognostic impact of baseline plasma metabolomics in DLBCL patients;

3. MATERIALS AND METHODS

3.1. Patients included in the study

The study cohort was consisted of 96 consecutive newly diagnosed DLBCL patients. This cohort of 96 patients treated at our institution and represented a subset of the cohort included in a previous genomic study from our group (Moia *et al.*, 2025). All patients were homogeneously treated with R-CHOP-based chemoimmunotherapy. Plasma samples were collected before the 1st cycle in Streck BCT tubes. Patients were fasting for at least 6 hours before blood sampling. Patients provided informed consent in accordance with Institutional Review Board requirements and the Declaration of Helsinki. The study was approved by the Ethical Committee of the Ospedale Maggiore della Carita di Novara associated with the Universita del Piemonte Orientale (study number CE 120/19).

3.2. Separation of granulocytes from peripheral blood (PB)

Peripheral blood (PB) granulocytes were isolated using Ficoll gradient density centrifugation to obtain normal germline genomic DNA (gDNA). The PB was diluted at 1:2 ration with physiological saline (0.9% NaCl) and centrifuged at 1800 rpm for 25 minutes using Sigma Diagnostic™ Histopaque ®-1077 Cell Separation Medium (Sigma-Aldrich, St.Louis, MO, USA) to separate granulocytes from mononuclear cells (monocytes and lymphocytes).

3.3. Extraction of normal gDNA

Normal gDNA was extracted using the “salting out” method (Miller *et al.*, 1988). Cells were lysed with a Lysis Buffer containing Tris-HCl 1M (pH 8.2), NaCl 5M, and EDTA 0.5M, along with 20% sodium dodecyl sulfate (SDS), and then digested with 20 mg/ml proteinase enzyme (pronase E). The samples were incubated overnight at 37^{0}C in a shaking incubator. Proteins were precipitated by adding 6M NaCl and removed after centrifugation at 3200 rpm for 20 minutes. DNA was then precipitated using pure ethanol, forming a milky, jelly-like substance which was collected with glass loops and washed 3 times using 75% ethanol. After

evaporating the residual ethanol, the DNA was dissolved in TE Buffer (Tris-HCl 1M, pH 8.2, EDTA 0.5M).

3.4. Plasma ctDNA extraction

PB samples were collected in Cell-DNA BCT® tubes and centrifuged at 800 relative centrifugal force (RCF) for 10 minutes at 4^0C to separate plasma from blood cells. The plasma was then centrifuged again at 13000 rpm for 10 minutes at 4^0C to remove any remaining cells. Plasma samples were stored at -80^0C until DNA extraction. ctDNA was extracted from 2-3 ml plasma aliquots immediately after thawing, using the Maxwell ® RSC LV ccfDNA Kit Custom (Promega Corporation, Madison, WI, USA). Quantification was performed with a Quantus Fluorometer using the QuantiFluor double-stranded DNA (dsDNA) System (Promega Corporation). The quality of the extracted ctDNA was evaluated with the 2100 Bioanalyzer Instrument (Agilent Technologies, Santa Clara, CA, USA).

3.5. DNA quantification and fragmentation

gDNA was quantified using the Quant-iT^{TM} PicoGreen dsDNA Assay kit (ThermoFisher Scientific, Eugene, OR, USA). PicoGreen is a dye that selectively binds to dsDNA, enabling an accurate measurement of DNA quantity. Fluorescence readings were taken with the Infinite F200 fluorometer (TECAN, Mannedorf, Switzerland) using Magellan software. Measurements were made at an excitation wavelength of 485 nm and emission wavelength of 530 nm. A standard curve was generated by preparing serial 1:2 dilutions of DNA with known concentration. The Quant-iT^{TM} PicoGreen assay was performed at 1:200 dilution.

gDNA was extracted from tissue samples and were sheared by sonication using the M220 focused ultrasonicator (Covaris®, Woburn, MA, USA) before library preparation to produce DNA fragments of 250-300 base pairs. Fragment sizes were verified with the 2100 Bioanalyzer Instrument. In contrast, circulating tumor DNA (ctDNA) is naturally fragmented and was used directly for library construction without further fragmentation.

3.6. Library design for hybrid selection

A targeted re sequencing gene panel was specifically designed for this research project, covering the coding exons and splice sites of 109 genes (total target region: 199411 base pairs) that are frequently mutated in DLBCL and other B-cell malignancies.

3.7. CAPP-seq library preparation

The gene panel was analyzed in two sample types: i) plasma ctDNA collected at diagnosis; and ii) germline gDNA from matched granulocytes for comparison. NGS libraries were prepared using the KAPA HyperPrep Library Preparation Kit (KAPA Biosystems, Wilmington, MA, USA), with hybrid selection performed using the custom KAPA HyperChoice probes (Roche, Basel, Switzerland). Multiplexed libraries were sequenced using 300-bp paired end runs on MiSeq Illumina platform (San Diego, CA, USA).

3.8. Metabolomic analysis

For the metabolomic analysis, blood samples were prepared following a protocol already published by Barberis et al. (Barberis *et al.*, 2020). Small molecules were extracted from 30µL of plasma and then derivatized following a methoximation and sialylation process. Subsequently, an untargeted metabolomic approach was performed using a LECO Pegasus BT 4D two-dimensional gas chromatography-time of flight mass spectrometry (GCxGC/TOFMS) equipped with a LECO dual-stage quad jet thermal modulator (Leco Corporation., St. Josef, MI). ChromaTOF version 5.51 was used for the raw data processing. Metabolites were then annotated using commercial and customized mass spectral libraries (NIST, Mainlib, Replib and Fiehn) (Kind *et al.*, 2009).

Putative biomarkers were selected to be verified for their identity and to assess their concentrations by evaluating authentic standards. Samples of this study cohort were analyzed using a high resolution (HR) instrument, a GCxGC/HRT-TOFMS. Retention times, retention indexes and fragmentation spectra were then compared to allow the identification of molecules and data elaboration was performed using ChromaTOF software.

3.9. GCxGC/TOFMS analysis

For the metabolomics analysis, a LECO Pegasus BT 4D, a two dimensional gas chromatography-time of flight mass spectrometry GCxGC/TOFMS equipped with a LECO dual-stage quad jet thermal modulator was used (Leco Corporation., St. Josef, MI). The first-dimension column was a 30m long Rxi-5Sil MS capillary column (Restek Corporation., Bellefonte, PA) with an internal diameter of 0.25 mm and a stationary phase film thickness of 0.25µm. The secondary column was a 2m long Rxi-17Sil MS (Restek Corporation., Bellefonte, PA) with the same diameter and thickness parameters of the first column. The carrier gas of choice was high-purity helium (99.9999%) used a flow rate of 1.4 mL/min. As previously reported by Barbies et al. (Barberis *et al.*, 2020), samples were analyzed using injecting 1µL of sample at 250^0C in splitless mode. The temperature program was as follows: the initial temperature was set at 70^0C for 2 min, increased by 6^0C/min up to 160^0C, then 10^0C/min up to 240^0C, and 20^0C/min to 300^0C and finally held for 6 min. The secondary oven was kept at $+20^0$C relative to the gas chromatography (GC) oven temperature of the first column. The programming rate was the same for both columns.

Electron impact ionization was applied (70eV). The ion source temperature was set at 250^0C, and the mass range was 25-550 m/z with an extraction frequency of 32 kHz. The acquisition rates were 200 spectra and the modulation period was 4 s throughout the entire run. The modulator temperature offset was $+15^0$C relative to the secondary oven temperature, while the transfer line was set at 280^0C. Chromatograms were acquired in total ion current (TIC) mode. Peaks with signal-to-noise (S/N) values lower than 500 were rejected. ChromaTOF version 5.51 was used for the raw data processing. Metabolites were then annotated using commercial mass psectral libraries (NIST, Mainlib, Replib and Fiehn). During the analyses, quality controls, prepared pooling all the patients' plasma, and blank samples were run daily in order to check for system suitability. Internal standards (deuterated tridecanoic acid, palmitic and stearic acids and hexadecane) were spiked in each sample during preparation and were used to monitor instrument stability and for data normalization, which also included a Lowess normalization. The statistical analysis was performed through Metaboanalyst 6.0 online software.

3.10. Sample preparation for metabolomic analysis

For the metabolomics analysis, 30 µL of plasma were mixed with 1 ml of an CAN/IPA/H20 solution (3:3:2) supplemented with deuterated internal standards at 0.5 mg/ml (Merck, Darmstad, Germany). Each sample was vortexed, centrifuged at room temperature for 15 min at 14500xg and the supernatant was then dried in a speed-vacuum (ScanVac, LaboGene, Denmark). To perform the analysis of metabolites, samples were derivatized following a methoximation and sialylation process (20 µL of methoxamine, 80^0C, 20 min and 90 µL of BSTFA, 80^0C, 20 min) (Merck). Finally, the internal standard hexadecane was added and samples were ready to be injected for the GCxGC/TFOMS analysis.

3.11. Molecular characterization of the DLBCL cohort on ctDNA

The LyV4.0 CAncer Personalized Profiling by deep Sequencing Assay (CAPP-seq) was used for the study and comprised a panel of 109 genes (199411 bp) known to be relevant in DLBCL based on previous studies (Barberis *et al.*, 2020; Wright *et al.*, 2020a). The number of the libraries loaded in the MiSeq/NextSeq550 instruments was tailored to obtain at least a coverage >2000x in >80% of the region of interest. A background error-suppressed approach was used for variant calling. The limit of quantification of the LyV4.0 CAPP-seq assay was 0.09%, which represented the analytical background noise threshold over which the assay produced a signal distinguishable from “blank”. The analytical sensitivity of the LyV4.0 CAPP-seq was 0.1%, representing the smallest detectable allele frequency. Copy-number analysis was performed using the CNVkit software toolkit (version 0.9.10) in Python 3.11.4 (Talevich *et al.*, 2016).

ctDNA levels were reported as haploid genome equivalents per ml of plasma (hGE/mL), determined as the product of total cell-free DNA (cfDNA) concentration and the mean allele fraction of somatic mutations. This value was expressed as a base-10 logarithm (log hGE/mL) (Kurtz *et al.*, 2018).

The DLBclass tool was used to classify the DLBCL cases of the study cohort into genetics subtypes (Chapuy *et al.*, 2025). A LASSO-based ensemble feature selection is utilized to find potential correlations between metabolites and each molecular cluster.

A reference file was built from 31 minimal residual disease-negative samples; read depths were median-centered and bias-corrected (GC-content, sequence repeats, target

density) to produce normalized $\log_2$ read depth values for each bin. The results of CNVkit were internally validated by comparison to ichorCNA (Rothwell *et al.*, 2019). Finally, GISTIC algorithm was applied on the segmented data using the GISTIC2.0 GenePattern module (version 6.15.30) to identify statistically significant copy number abnormalities (CNAs) (Beroukhim *et al.*, 2007).

3.12. Statistical Analysis

The primary clinical endpoint was progression-free survival (PFS). An elastic net penalized Cox regression model was fitted to identify plasma metabolites associated with PFS by using the glmnet package in RStudio. The maximally selected rank statistics was used to identify the best cut-off values in predicting PFS for selected metabolites. Survival analysis was performed using the Kaplan-Meier method and compared between strata using the Log-rank test. The nonparametric tree modelling technique of classification and regression tree (CART) analysis was also used to group risk classes according to candidate metabolites and ctDNA levels. Chi-square and Mann-Whitney tests were used to compare dichotomous and continuous variables, respectively. All the statistical analysis were performed with the Statistical Package for the Social Sciences (SPSS) software v.24.0 (Chicago, IL) and RStudio Version 1.2.1335 2009-2019, Inc. Moreover, Statistical significance was defined as p-value <0.05.

4. RESULTS

4.1. Characteristics of study participants

In the study cohort, the median age was 68 years, 71 (74.0%) patients presented an Ann Arbor stage III/IV and 56 (58.3%) patients presented and International Prognostic Index (IPI) ≥ 3 (Table 1).

After a median follow-up of 55.6 months, the 56-month Progression-free survival (PFS) and overall survival (OS) were 59.9% (95% CI 50.5%-71.0%) and 69.4% (95% CI 60.2%-80.1%), respectively (Figure 2A, B).

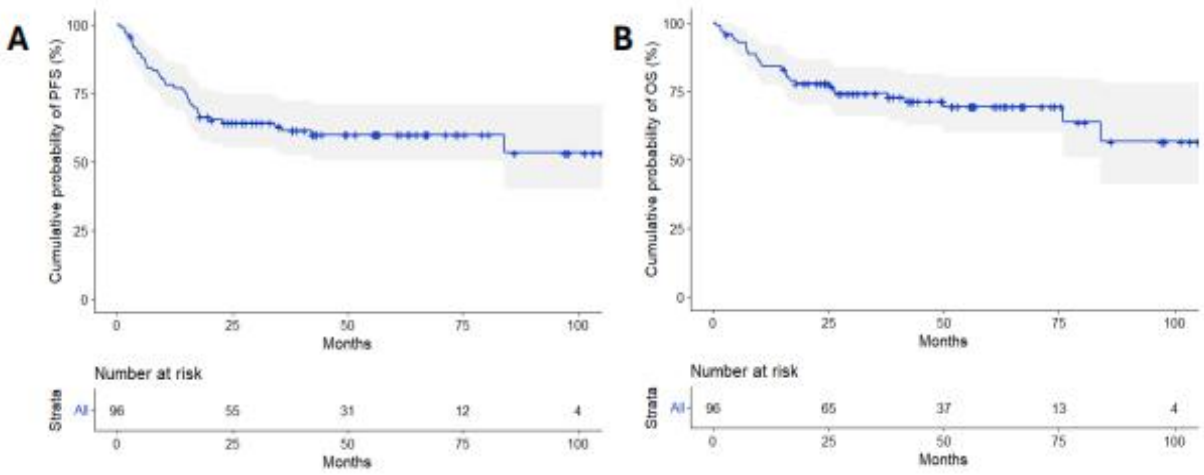


Figure 2 - Kaplan-Meier curves of (A) PFS and (B) OS of the 96 DLBCL patients included in the study cohort.

Table 1 Patients Characteristics

Characteristics	Study Cohort (N=96)
Median Age	**68 (IQR 54-76)**
I	10 (10.4%)
II	15 (15.6%)
III	11 (11.5%)
IV	60 (62.5%)
IPI	
0-1	21 (21.9%)
2	19 (19.8%)
3	23 (23.9%)

4-5	33 (34.4%)
COO	
GC	29 (30.2%)
Non-GC	56 (58.3%)
Not available	11 (11.5%)
LDH above ULN	
Yes	59 (61.5%)
No	37 (38.5%)
Extranodal Sites	
Yes	60 (62.5%)
No	36 (37.5%)

IPI, international prognostic index; COO, cell of origin; GC, germinal center; LDH, lactate dehydrogenase; ULN, upper limit of normal.

After a median follow-up of 58.8 months, the 56-month PFS and OS were 51.3% (95% CI 42.7%-73.6%), respectively (Table 1).

ctDNA CAPP-Seq analysis identified *PIM1* as the most frequent gene mutation, present in 21 (21.9%) patients, followed by *MYD88* in 18 (18.8%) and *KMT2D* in 18 (18.8%) patients. The complete molecular characterization of the study cohort, including both mutations and copy number variations (CNVs), is presented in Figure 3.

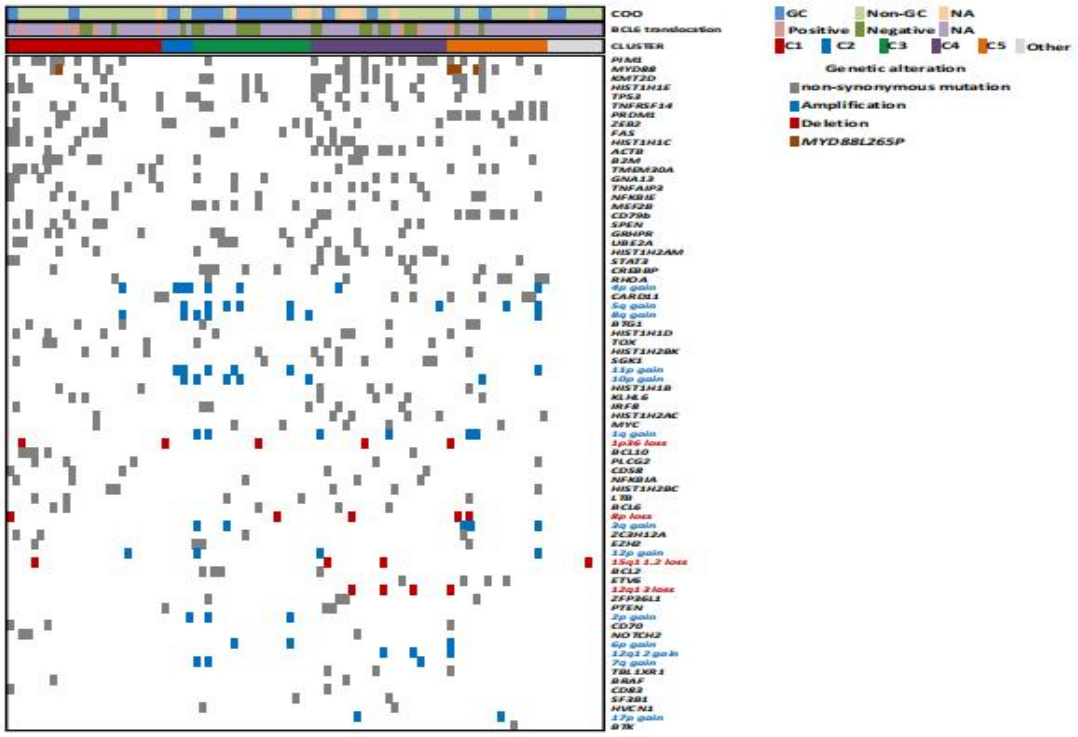


Figure 3- Molecular characterization of the study cohort on ctDNA.

4.2. Association between metabolomic profile of the study cohort, cell of origin and molecular clusters

The metabolomic profiling allowed the identification of a total of 280 metabolites and small molecules, ranging from amino acids and their derivatives to organic and fatty acids and sugars. The association between the metabolomic profile and COO was evaluated in 85 of 96 patients for whom the COO based on the Hans algorithm was available. No metabolite significantly associated with COO status .

The DLBclass algorithm classified 87 (90.6%) patients of the study cohort into a molecular cluster as follows: 25 patients to cluster C1, 5 to C2, 19 to C3, 22 to C4, 16 to C5.

Hierarchical clustering grouped C1 with C3 and C2 with C5, whereas C4 formed a separate branch and displayed the most distinct overall coefficient profile. The reporting criterion of the ridge-based model was met by 36 metabolites for C1, 26 for C2, 10 for C3, 40 for C4 and 10 for C5, yielding 122 cluster-metabolite associations, which represented 96 unique metabolites (Figure 4A and B). 74 were specific to one cluster, 18 were shared by two clusters and 4 by three clusters; no metabolite was shared across four or all five clusters. Furthermore, bootstrap resampling identified 15 associations with stability of at least 0.60 (Figure 4C).

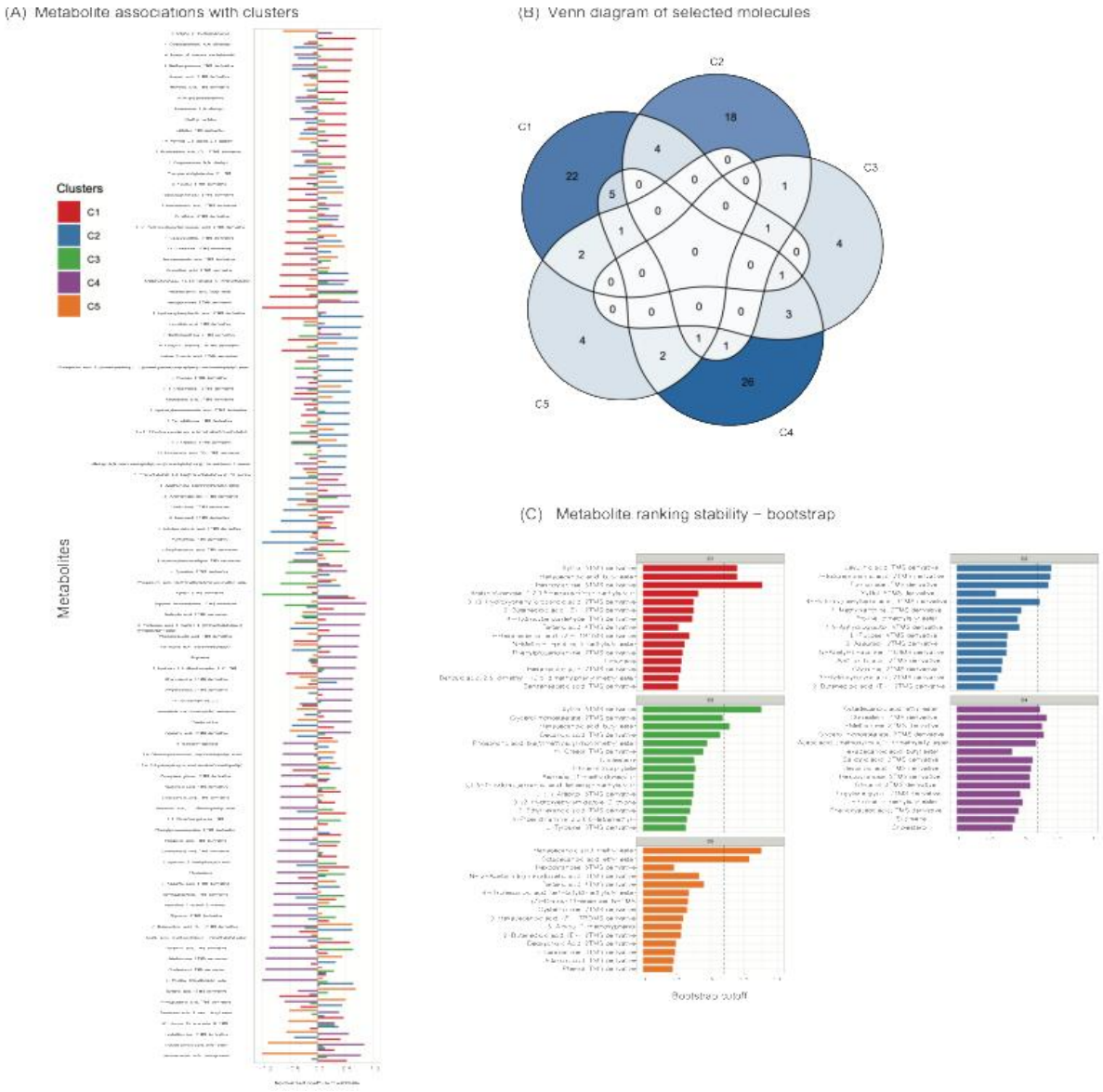


Figure 4- Metabolite associations with molecular clusters. (A) Normalized ridge coefficients for the 96 metabolites reaching the reporting threshold in at least one cluster. (B) Venn diagram of these metabolites by cluster (74 specific to one cluster, 18 shared by two, 4 shared by three). (C) Bootstrap selection stability per metabolite (proportion of 500 resamples meeting the threshold).

Pathway analysis revealed nominal enrichment of several metabolic processes across the identified clusters. However, given the limited cluster sizes, these findings should be interpreted as hypothesis-generating. Cluster C1 was mainly enriched in pathways related to fatty acid biosynthesis, phenylalanine, and pentose and glucoronate interconversions (Figure 5A). Cluster C2 showed an enrichment in pathways involved in pentose and glucoronate interconversions and in tryptophan metabolism (Figure 5B). Cluster C3 presented pathways involved in fatty acid biosynthesis, pentose and glucoronate interconversions and tyrosine metabolism (Figure 5C). Cluster C4 was characterized by pathways linked to fatty acid

biosynthesis (Figure 5D), while cluster C5 exhibited an enrichment in glyoxylate and dicarboxylate metabolism and in fatty acid biosynthesis (Figure 5E).

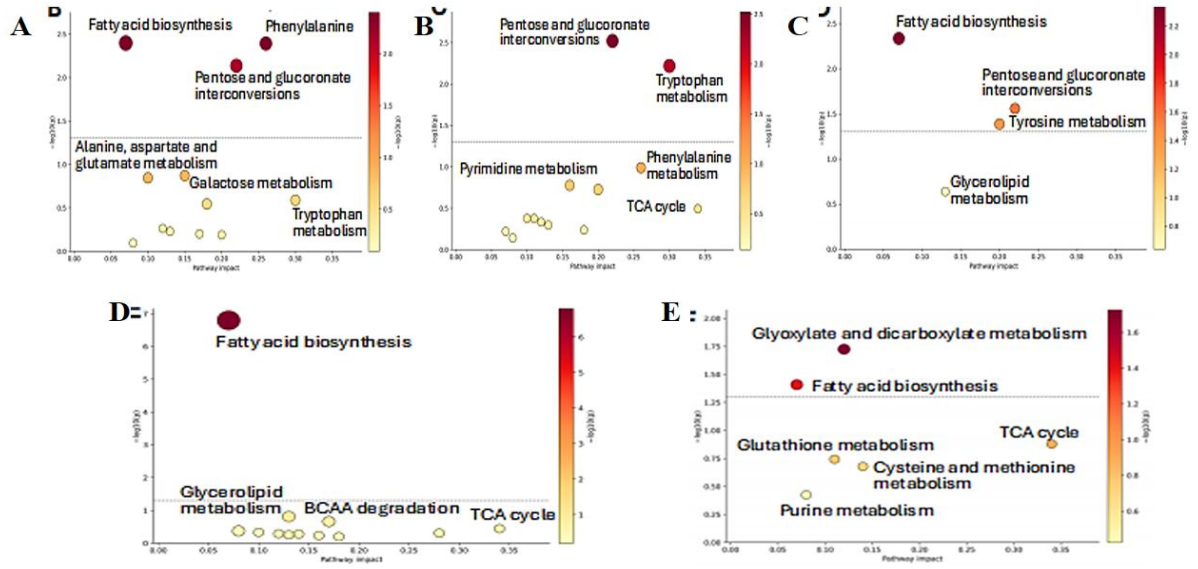


Figure 5- Metabolomics signature and pathway enrichment analysis of DLBCL patients according to molecular clustering.

4.3. 2-hydroxubutyric acid (2HB) associates with poor outcomes in the study cohort

Among the 280 compounds identified by untargeted metabolomic profiling and considered as continuous variables, elastic net Cox regression analysis identified 2-hydroxybutyric acid (2HB) and isopropyl stearate as potential PFS-associated metabolites. Because isopropyl stearate is not recognized as an endogenous human metabolite in major metabolomic databases, including the Human Metabolome Database (HMDB) and the Kyoto Encyclopedia of Genes and Genomes (KEGG), and since it lacks evidence of association with human metabolic pathways or metabolomic profiles, it was excluded from subsequent survival analyses.

Recursive partitioning was used to maximize the log-rank statistics for PFS for 2HB abundance values of the 96 patients enrolled in the study cohort. The optimal abundance cut-off for 2HB was 413.83.

Patients with higher 2HB abundance values (>413.83, N=20) displayed a 56-month PFS and OS of 31.5% (95% CI 15.6%-63.7%) and 45.1% (95% CI 26.6%-76.7%) compared to 67.3% (95% CI 57.3%-79.0%) and 75.6% (95% CI 65.9%-86.7%) in patients with lower

values (≤413.83, N=76), respectively (p=0.0047 and p=0.0035, respectively) (Figure 6A and B). The C-index based on 2HB abundance levels was 0.587 for PFS and 0.602 for OS.

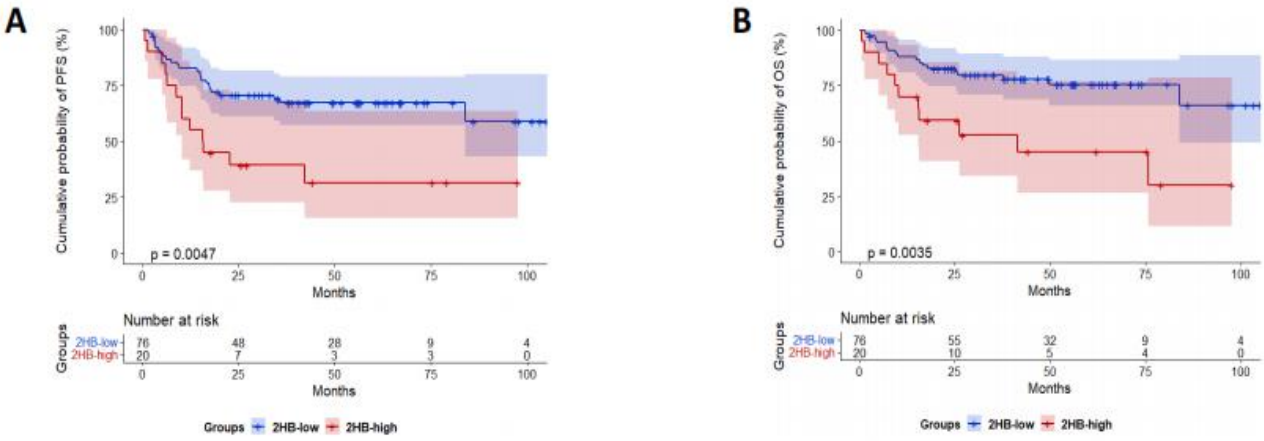


Figure 6 - Kaplan-Meier curves for PFS and OS showing 2HB and ctDNA prognostic impact in the study cohort. (A) PFS impact of 2HB levels. (B) OS impact of 2HB levels.

According to bivariate correlation analysis, no significant associations were observed between 2HB levels and age at diagnosis (p=0.349), COO (p=0.133), IPI (p=0.737), elevated LDH (p=0.632), and Ann Arbor stage (p=0.853) in the study cohort. Also, comparison of categorical variables did not show statistically significant difference between 2HB-high and 2HB-low patients in the distribution of non-GC DLBCL, IPI ≥ 3, elevated LDH and advanced Ann Arbor stage (stages III and IV). Also, we investigated potential associations between elevated 2HB levels and other patient characteristics, including body mass index (BMI) ≥ 30 Kg/m^2 (p=0.378), statin (p=0.833) and metformin (p=0.836) use, and the presence of diabetes (p=0.003) at the time of lymphoma diagnosis. The presence of diabetes associated with elevated 2HB levels but, importantly, diabetes itself did not correlate with shorter PFS or OS (p=0.248 and p=0.586, respectively). Furthermore, elevated 2HB levels (HR 2.45, 95% CI 1.21-4.97, p=0.013) maintained an independent association with shorter PFS when adjusted for diabetes at lymphoma diagnosis (HR 1.21, 95% CI 0.48-3.04, p=0.685).

5. DISCUSSION

This present study demonstrated an unbiased discovery approach that enabled the identification of a specific circulating metabolite as novel prognostic biomarker for newly diagnosed DLBCL. Overall, the DLBCL metabolomic profile demonstrates to differ across DLBclass molecular clusters. 2HB independently associates with worse outcome and refines the prognostic accuracy of plasma ctDNA levels, potentially providing information which are not captured by the liquid biopsy. Moreover, 2HB can be defined as a byproduct of amino acid catabolism and glutathione synthesis, while linking to oxidative stress and altered redox activity, preferably in hypoxic conditions.

DLBCL is characterized by marked molecular heterogeneity, and findings of this study indicate that metabolic heterogeneity represents an additional reflection of disease complexity. Futhermore, no metabolite was associated with the COO, suggesting that metabolomic alterations do not simply mirror COO-defined transcriptional programs. In contrast, regression analyses revealed cluster-specific metabolic signatures across DLBclass subtypes, confirming that tumor molecular programs may shape the systemic metabolic context (Shi *et al.*, 2024; Catalano *et al.*, 2025; Ling *et al.*, 2025). The absence of overlapping between the cluster-associated metabolites and the prognostic metabolite 2-HB further suggests that these biomarkers are not merely surrogates of molecular subtype but, rather, reflect broader tumor-host interactions. Whether the different molecular clusters drive a various metabolomics profile, or vice versa, still remains to be clarified.

Furthermore, the cluster-specific metabolic processes were identified from analysis of this approach that partially reflect the oncogenic related mechanisms of each DLBclass subtype. According to that, fatty acid biosynthesis mechanisms were demonstrated in both C1 and C3 clusters, while tryptophan metabolism alterations were represented in C2 cluster type which was consisted of immunomodulatory aspect of tryptophan catabolism in B-cell malignancies. Moreover, cluster 4 was predominantly characterized by the fatty acid biosynthesis, while cluster 5 represented metabolism related to glyoxylates and dicarboxylates. These metabolic distinctions through the molecular clusters further underscore the essential differences in the genomic and metabolic concepts according to the previous studies (Chapuy, Stewart, Andrew J Dunford, Kim, Kamburov, Staiger, *et al.*, 2018; Wright *et al.*, 2020b; Chapuy *et al.*, 2025).

The mechanism through which 2-HB predicts poor prognosis in DLBCL remain to be elucidated in a better detailed version. The plasma levels of 2-HB plasma are strongly

associated with pancreatic β-cell dysfunction and increased free fatty acids production. Accordingly, this metabolite has been linked to the conditions related to the systemic inflammation, oxidative stress, and insulin resistance (Sousa *et al.*, 2021; Wang *et al.*, 2023), highlighting the potential role of these aspects as risk factors for the development and progression of both solid and hematological malignancies.

Furthermore, 2-HB has been identified as a gut microbiome-derived metabolite, supporting the potential involvement of the microbiome in modulating the immune system and promoting DLBCL growth and progression (Lin *et al.*, 2023; Casadei *et al.*, 2024). Whether microbiome-derived metabolites contribute to the treatment response in DLBCL deserves further investigation, particularly in patients receiving T-cell redirecting therapies (Hu *et al.*, 2022; Stein-thoeringer *et al.*, 2023; Uribe-herranz *et al.*, 2023).

In the present study, metabolomic analyses were performed only on plasma samples, which did not allow to clearly determine the origin of specific metabolites, particularly the potential microbiome origin of 2-HB. Stool samples are defined as the inclusion of additional biological samples, combined with *in vitro* assays, will be necessary to definitively confirm the origin of certain metabolites and to further exploration of the microbiome-lymphoma interactions to be done.

Additionally, the present study was consisted of several limitations to be acknowledged. This study cohort composed of 96 newly diagnosed DLBCL patients with a single center for the treatment, while revealing a well-structured and homogeneously treated population. Furthermore, the metabolomic analysis was performed exclusively on the plasma samples, but the precise analysis and evaluation of the cellular and tissue characterization of the identified metabolites were not detected by these plasma samples, particularly in the case of 2-HB metabolite.

Plasma 2-HB is a novel, host-derived prognostic biomarker in newly diagnosed DLBCL, that could be integrated in the future with other DLBCL biomarker to further enhance disease risk stratification.

6. BIBLIOGRAPHY

Alaggio, R. *et al.* (2022) 'The 5th edition of the World Health Organization Classi fi cation of Haematolymphoid Tumours : Lymphoid Neoplasms', (June). doi: 10.1038/s41375-022-01620-2.

Alizadeh, A. A. *et al.* (2000) 'Distinct types of diffuse large B-cell lymphoma identi ® ed by gene expression pro ® ling', 403(February).

Almasri, M. *et al.* (2025) 'Liquid Biopsy in B and T Cell Lymphomas : From Bench to Bedside', pp. 1–23.

Barberis, E. *et al.* (2020) 'Large-Scale Plasma Analysis Revealed New Mechanisms and Molecules Associated with the Host Response to SARS-CoV-2'.

Barrans, S. *et al.* (2010) 'J OURNAL OF C LINICAL O NCOLOGY Rearrangement of MYC Is Associated With Poor Prognosis in Patients With Diffuse Large B-Cell Lymphoma Treated in the Era of Rituximab Not known', 28(20). doi: 10.1200/JCO.2009.26.3947.

Barrans, S. L. *et al.* (2003) 'The t (14 ; 18) Is Associated with Germinal Center-derived Diffuse Large B-Cell Lymphoma and Is a Strong Predictor of Outcome 1', 9(June), pp. 2133–2139.

Basso, K. and Dalla-favera, R. (2015) 'Germinal centres and B cell lymphomagenesis E l', *Nature Publishing Group*, 15(March), pp. 172–184. doi: 10.1038/nri3814.

Bereshchenko, O. R., Gu, W. and Dalla-favera, R. (2002) 'Acetylation inactivates the transcriptional repressor BCL6', 32(december), pp. 606–613. doi: 10.1038/ng1018.

Beroukhim, R. *et al.* (2007) 'Assessing the significance of chromosomal aberrations in cancer : Methodology and application to glioma', 104(50), pp. 20007–20012.

Boice, M. *et al.* (2016) 'Loss of the HVEM tumor suppressor in lymphoma and restoration by modified CAR-T cells', 167(2), pp. 405–418. doi: 10.1016/j.cell.2016.08.032.Loss.

Bojarczuk, K. *et al.* (2019) 'Targeted inhibition of PI3Ka/d is synergistic with BCL-2 blockade in genetically defined subtypes of DLBCL', *Blood*, 133(1), pp. 70–80. doi: 10.1182/blood-2018-08-872465.

Boone, D. L. *et al.* (2004) 'The ubiquitin-modifying enzyme A20 is required for termination of Toll-like receptor responses', 5(10), pp. 1052–1060. doi: 10.1038/ni1110.

Casadei, B. *et al.* (2024) 'treated with checkpoint inhibitors — The MicroLinf Study', (July), pp. 1–12. doi: 10.1002/hon.3301.

Catalano, M. *et al.* (2025) 'Navigating Cancer Complexity : Integrative Multi-Omics Methodologies for Clinical Insights'. doi: 10.1177/11795549251384582.

Cattoretti, G. *et al.* (2009) 'Targeted disruption of the S1P2 sphingosine 1-phosphate receptor

gene leads to diffuse large B-cell lymphoma formation', 69(22), pp. 8686–8692. doi: 10.1158/0008-5472.CAN-09-1110.Targeted.

Challa-malladi, M. *et al.* (2011) 'Article Combined Genetic Inactivation of b 2-Microglobulin and CD58 Reveals Frequent Escape from Immune Recognition in Diffuse Large B Cell Lymphoma', *Cancer Cell*, 20(6), pp. 728–740. doi: 10.1016/j.ccr.2011.11.006.

Chapuy, B., Stewart, C., Dunford, Andrew J, Kim, J., Kamburov, A., Redd, R. A., *et al.* (2018) 'mechanisms and outcomes', 24(May). doi: 10.1038/s41591-018-0016-8.

Chapuy, B., Stewart, C., Dunford, Andrew J, Kim, J., Kamburov, A., Staiger, A. M., *et al.* (2018) 'Molecular Subtypes of Diffuse Large B-cell Lymphoma are Associated with Distinct Pathogenic Mechanisms and Outcomes', 24(5), pp. 679–690. doi: 10.1038/s41591-018-0016-8.Molecular.

Chapuy, B., Stewart, C., Dunford, Andrew J., *et al.* (2018) 'Molecular subtypes of diffuse large B cell lymphoma are associated with distinct pathogenic mechanisms and outcomes', *Nature Medicine*, 24(5), pp. 679–690. doi: 10.1038/s41591-018-0016-8.

Chapuy, B. *et al.* (2025) 'LYMPHOID NEOPLASIA DLB class : a probabilistic molecular classi fi er to guide clinical investigation and practice in diffuse large B-cell lymphoma', *BLOOD*, 145(18), pp. 2041–2055. doi: 10.1182/blood.2024025652.

Chiappella, A. *et al.* (2013) 'prednisone and rituximab is safe and effective in untreated , elderly patients with diffuse large B-cell lymphoma : a phase I study by the Fondazione Italiana Linfomi', 98(11). doi: 10.3324/haematol.2013.085134.

Compagno, M. *et al.* (2009) 'Mutations of multiple genes cause deregulation of NF-kB in diffuse large B-cell lymphoma', 459(7247), pp. 717–721. doi: 10.1038/nature07968.Mutations.

Czermin, B. *et al.* (2002) 'Drosophila Enhancer of Zeste / ESC Complexes Have a Histone H3 Methyltransferase Activity that Marks Chromosomal Polycomb Sites', 111, pp. 185–196.

Diaz, L. A. and Bardelli, A. (2014) 'Liquid Biopsies : Genotyping Circulating Tumor DNA', 32(6). doi: 10.1200/JCO.2012.45.2011.

Dominguez-sola, D. *et al.* (2015) 'The FOXO1 Transcription Factor Instructs the Germinal Center Dark Zone Program Article The FOXO1 Transcription Factor Instructs the Germinal Center Dark Zone Program', *Immunity*, 43(6), pp. 1064–1074. doi: 10.1016/j.immuni.2015.10.015.

Dondolin, R. *et al.* (2025) 'Integration of [18 F] FDG-PET radiomics with liquid biopsy improves outcome prediction in newly diagnosed diffuse large B-cell lymphoma', *Leukemia*, (February). doi: 10.1038/s41375-025-02688-2.

Dunleavy and Wilson (2014) 'HHS Public Access', 28(4), pp. 326–334.

Edeiros, L. J. E. M. (2018) 'REVIEW : 50TH ANNIVERSARY ISSUE Diffuse large B-cell lymphoma', 50(January), pp. 74–87. doi: 10.1016/j.pathol.2017.09.006.

Fei, F. *et al.* (2022) 'Plasma Metabolites Forecast Occurrence and Prognosis for Patients With Diffuse Large B-Cell Lymphoma', 12(June), pp. 1–11. doi: 10.3389/fonc.2022.894891.

Flowers, C. *et al.* (2022) 'ABCL-073 Polatuzumab Vedotin Plus Rituximab, Cyclophosphamide, Doxorubicin, and Prednisone (Pola-R-CHP) Versus Rituximab, Cyclophosphamide, Doxorubicin, Vincristine and Prednisone (R-CHOP) Therapy in Patients With Previously Untreated Diffuse Large B-Cell', *Clinical Lymphoma, Myeloma and Leukemia*, 22(October), pp. S358–S359. doi: 10.1016/S2152-2650(22)01498-7.

Green, J. A. and Cyster, J. G. (2012) 'S1PR2 links germinal center confinement and growth regulation', 247(1), pp. 36–51. doi: 10.1111/j.1600-065X.2012.01114.x.S1PR2.

Grommes, C. *et al.* (2017) 'Ibrutinib Unmasks Critical Role of Bruton Tyrosine Kinase in Primary CNS Lymphoma'. doi: 10.1158/2159-8290.CD-17-0613.

He, R. *et al.* (2026) 'A panoramic study of circulating tumor DNA in diffuse large B-cell lymphoma', *Genes & Diseases*, p. 102038. doi: 10.1016/j.gendis.2026.102038.

Heitzer, E., Roberts, C. E. S. and Speicher, M. R. (2019) 'Current and future perspectives of liquid biopsies in genomics-driven oncology', *Nature Reviews Genetics*, 20(February). doi: 10.1038/s41576-018-0071-5.

Hu, Y. *et al.* (2022) 'CAR-T cell therapy-related cytokine release syndrome and therapeutic response is modulated by the gut microbiome in hema- tologic malignancies'. doi: 10.1038/s41467-022-32960-3.

Iqbal, J. *et al.* (2007) 'NIH Public Access', 21(11), pp. 2332–2343.

Karube, K. *et al.* (2018) 'Integrating genomic alterations in diffuse large B-cell lymphoma identi fi es new relevant pathways and potential therapeutic targets', (July 2017), pp. 675–684. doi: 10.1038/leu.2017.251.

Kato, M. *et al.* (2009) 'Frequent inactivation of A20 in B-cell lymphomas', *Nature*, 459(June). doi: 10.1038/nature07969.

Kind, T. *et al.* (2009) 'mass spectral and retention index libraries for metabolomics based on quadrupole and time-of-flight gas chromatography/mass spectrometry', 81(24), pp. 10038–10048. doi: 10.1021/ac9019522.FiehnLib.
Kurtz, D. M. *et al.* (2018) 'Circulating tumor DNA measurements as early outcome predictors in diffuse large B-cell lymphoma', *Journal of Clinical Oncology*, 36(28), pp. 2845–2853. doi: 10.1200/JCO.2018.78.5246.

Kwak, J. (2012) 'Treatment of Diffuse Large B Cell Lymphoma', pp. 369–377.

Lacy, S. E. *et al.* (2020) 'Targeted sequencing in DLBCL, molecular subtypes, and outcomes: A Haematological Malignancy Research Network report', *Blood*, 135(20), pp. 1759–1771. doi: 10.1182/BLOOD.2019003535.

Lin, Z. *et al.* (2023) 'The gut microbiota correlate with the disease characteristics and

immune status of patients with untreated diffuse large B-cell lymphoma', (February), pp. 1–11. doi: 10.3389/fimmu.2023.1105293.

Ling, B. *et al.* (2025) 'Integrative Multi-Omics Analysis Reveals Key Metabolic Regulators and Prognostic Biomarkers in Pediatric and Adult Thyroid Cancer', 16. doi: 10.7150/jca.117034.

Lionakis, M. S. *et al.* (2017) 'Inhibition of B Cell Receptor Signaling by Ibrutinib in Primary Central Nervous System Lymphoma', 31(6), pp. 833–843. doi: 10.1016/j.ccell.2017.04.012.Inhibition.

Liu, Y. and Barta, S. K. (2019) 'Diffuse large B-cell lymphoma : 2019 update on diagnosis , risk stratification , and treatment', (January), pp. 604–616. doi: 10.1002/ajh.25460.

Lyon-sud, C. H. and Lyon, H. C. De (2016) 'Diffuse large B-cell lymphoma : R-CHOP failure — what to do ?', pp. 366–378.

Martinez, L. Q. (2017) 'The 2016 updated WHO classification of lymphoid neoplasias', 35, pp. 37–45. doi: 10.1002/hon.2399.

Mathews, L. A. *et al.* (2014) 'High-throughput combinatorial screening identifies drugs that cooperate with ibrutinib to kill activated B-cell – like diffuse large B-cell lymphoma cells', 111(6). doi: 10.1073/pnas.1311846111.
Mesin, L., Ersching, J. and Victora, G. D. (2016) 'Germinal Center B Cell Dynamics', *Immunity*, 45(3), pp. 471–482. doi: 10.1016/j.immuni.2016.09.001.

Mi, M. *et al.* (2021) 'Serum metabolomic profiling based on GC / MS helped to discriminate Diffuse Large B-cell Lymphoma patients with different prognosis', 111(August). doi: 10.1016/j.leukres.2021.106693.

Miller, S. A. *et al.* (1988) 'A simple salting out procedure for extracting DNA from human nucleated cells.', 16(3), p. 55404.

Moia, R. *et al.* (2019) 'Liquid biopsy in lymphomas : a potential tool for refining diagnosis and disease monitoring'. doi: 10.20517/2394-4722.2019.020.

Moia, R. *et al.* (2025) 'Molecular clustering on ctDNA improves the prognostic strati fi cation of patients with DLBCL compared with ctDNA levels', 9(7). doi: 10.1182/bloodadvances.2024014136.

Montagne, A. *et al.* (2026) 'Risk stratification of patients with diffuse large B-cell lymphoma using plasma NMR-based metabolomics at diagnosis', *Blood Advances*, 10(2), pp. 358–366. doi: 10.1182/bloodadvances.2025017248.

Morin, R. D. *et al.* (2010) 'Somatic mutation of EZH2 (Y641) in Follicular and Diffuse Large B-cell Lymphomas of Germinal Center Origin', 42(2), pp. 181–185. doi: 10.1038/ng.518.Somatic.

Morin, R. D. *et al.* (2011) 'Frequent mutation of histone-modifying genes in non-Hodgkin lymphoma'. doi: 10.1038/nature10351.

Muppidi, J. R. *et al.* (2014) 'Loss of signaling via Gα13 in germinal center B cell-derived lymphoma', 516(7530), pp. 254–258. doi: 10.1038/nature13765.Loss.

Pasqualucci, L. *et al.* (2006) 'Inactivation of the PRDM1 / BLIMP1 gene in diff use large B cell lymphoma', 203(2), pp. 311–317. doi: 10.1084/jem.20052204.

Pasqualucci, L. *et al.* (2011) 'Articles Analysis of the coding genome of diffuse large B-cell lymphoma', *Nature Publishing Group*, 43(9). doi: 10.1038/ng.892.

Pasqualucci, L. and Dalla-favera, R. (2018) 'Genetics of di ff use large B-cell lymphoma', 131(21), pp. 2307–2319. doi: 10.1182/blood-2017-11-764332.

Phillips, T. J. *et al.* (2018) 'Phase 1 study of the PI3K d inhibitor INCB040093 6 JAK1 inhibitor itacitinib in relapsed / refractory B-cell lymphoma', 132(3), pp. 293–306. doi: 10.1182/blood-2017-10-812701.

Rosenthal, A. *et al.* (2017) 'High grade B-cell lymphoma with rearrangements of MYC and BCL2 and/or BCL6: Double hit and triple hit lymphomas and double expressing lymphoma', 31(2), pp. 37–42. doi: 10.1016/j.blre.2016.09.004.High.

Rosenwald, A. and Wright, G. et al (2002) 'THE USE OF MOLECULAR PROFILING TO PREDICT SURVIVAL AFTER CHEMOTHERAPY FOR DIFFUSE LARGE-B-CELL LYMPHOMA', 346(25).

Rossi, D. *et al.* (2017) 'Diffuse large B-cell lymphoma genotyping on the liquid biopsy', 129(14), pp. 1947–1957. doi: 10.1182/blood-2016-05-719641.

Rothwell, D. G. *et al.* (2019) 'Utility of ctDNA to support patient selection for early phase clinical trials : the TARGET study', *Nature Medicine*, 25(May). doi: 10.1038/s41591-019-0380-z.

Rui, L. *et al.* (2016) 'Epigenetic gene regulation by Janus kinase 1 in diffuse large B-cell lymphoma'. doi: 10.1073/pnas.1610970113.

Schiefer, A. *et al.* (2015) 'Impact of Single or Combined Genomic Alterations of TP53 , MYC , and BCL2 on Survival of Patients With Diffuse Large A Retrospective Cohort Study', 94(52), pp. 1–9. doi: 10.1097/MD.0000000000002388.

Schmidt *et al.* (2021) 'Metabolomics in Cancer Research and Emerging Applications in Clinical Oncology', 71(4), pp. 333–358. doi: 10.3322/caac.21670.Metabolomics.
Schmitz, R *et al.* (2018) 'Genetics and Pathogenesis of Diffuse Large B-Cell Lymphoma', 378(15), pp. 1396–1407. doi: 10.1056/NEJMoa1801445.Genetics.

Scott, D. W. *et al.* (2015) 'J OURNAL OF C LINICAL O NCOLOGY Prognostic Significance of Diffuse Large B-Cell Lymphoma Cell of Origin Determined by Digital Gene Expression in Formalin-Fixed Paraffin-Embedded Tissue Biopsies', 33(26). doi: 10.1200/JCO.2014.60.2383.

Sehn, L. H. and Salles, G. (2021) 'Diffuse Large B-Cell Lymphoma', 384(9), pp. 842–858.

doi: 10.1056/NEJMra2027612.Diffuse.

Sha, C. *et al.* (2019) 'Molecular high-grade B-cell lymphoma: Defining a poor-risk group that requires different approaches to therapy', *Journal of Clinical Oncology*, 37(3), pp. 202–212. doi: 10.1200/JCO.18.01314.

Shi, S. *et al.* (2024) 'Integrative Omics Analysis Reveals Metabolic Features of Ground-Glass Opacity-Associated Lung Cancer', 15. doi: 10.7150/jca.92437.

Shilatifard, A. (2012) 'NIH Public Access', (Figure 1), pp. 65–95. doi: 10.1146/annurev-biochem-051710-134100.The.

Silva, N. S. De and Klein, U. (2015) 'Dynamics of B cells in germinal centres', *Nature Publishing Group*, 15(March), pp. 137–148. doi: 10.1038/nri3804.

Sneeringer, C. J. *et al.* (2010) 'Coordinated activities of wild-type plus mutant EZH2 drive tumor-associated hypertrimethylation of lysine 27 on histone H3 (H3K27) in human B-cell lymphomas', 107(49), pp. 20980–20985. doi: 10.1073/pnas.1012525107.

Sousa, A. P. *et al.* (2021) 'Which Role Plays 2-Hydroxybutyric Acid on Insulin Resistance ?'
Stebegg, M. *et al.* (2018) 'Regulation of the Germinal Center Response', 9(October), pp. 1–13. doi: 10.3389/fimmu.2018.02469.

Stein-thoeringer, C. K. *et al.* (2023) 'A non-antibiotic-disrupted gut microbiome associated with clinical responses to CD19-CAR-T cell cancer immunotherapy', 29(4), pp. 906–916. doi: 10.1038/s41591-023-02234-6.A.
Steinberg, M. W., Cheung, T. C. and Ware, C. F. (2011) 'The Signaling Networks of the Herpesvirus Entry Mediator (TNFRSF14) in Immune Regulation', 244(1), pp. 169–187. doi: 10.1111/j.1600-065X.2011.01064.x.The.

Suman, A. F. *et al.* (2025) 'MYC and Metabolomics: Can We Use What We Know for DLBCL Subtyping and Diagnosis?', *Biomolecules*, 15(9), pp. 1–16. doi: 10.3390/biom15091346.

Talevich, E. *et al.* (2016) 'CNVkit : Genome-Wide Copy Number Detection and Visualization from Targeted DNA Sequencing', pp. 1–18. doi: 10.1371/journal.pcbi.1004873.

Talotta, D., Almasri, M. and Cosentino, C. (2023) 'Liquid biopsy in hematological malignancies : current and future applications', (April), pp. 1–10. doi: 10.3389/fonc.2023.1164517.

Thieblemont, C. *et al.* (2011) 'J OURNAL OF C LINICAL O NCOLOGY The Germinal Center / Activated B-Cell Subclassification Has a Prognostic Impact for Response to Salvage Therapy in Relapsed / Refractory Diffuse Large B-Cell Lymphoma : A Bio-CORAL Study', 29(31), pp. 4079–4087. doi: 10.1200/JCO.2011.35.4423.

Tilly, H. *et al.* (2015) 'Diffuse large B-cell lymphoma (DLBCL): ESMO Clinical Practice Guidelines for diagnosis, treatment and follow-up', *Annals of Oncology*, 26(Supplement 5), pp. vii78–vii82. doi: 10.1093/annonc/mdv304.

Tilly, H. (2022) 'Polatuzumab Vedotin in Previously Untreated Diffuse Large B_Cell Lymphoma', 386(4), pp. 351–363. doi: 10.1056/NEJMoa2115304.Polatuzumab.

Trinh, D. L. *et al.* (2013) 'Analysis of FOXO1 mutations in diffuse large B-cell lymphoma', 121(18), pp. 3666–3674. doi: 10.1182/blood-2013-01-479865.D.W.S.

Uribe-herranz, M. *et al.* (2023) 'Modulation of the gut microbiota engages antigen cross-presentation to enhance antitumor effects of CAR T cell immunotherapy', *Molecular Therapy*, 31(3), pp. 686–700. doi: 10.1016/j.ymthe.2023.01.012.

Visco, C. *et al.* (2012) 'Patients with diffuse large B-cell lymphoma of germinal center origin with BCL2 translocations have poor outcome, irrespective of MYC status: a report from an International DLBCL rituximab-CHOP Consortium Program Study', pp. 2–4. doi: 10.3324/haematol.2012.066209.

Visco, C. *et al.* (2020) 'Oncogenic mutations of MYD88 and CD79B in diffuse large B-cell lymphoma and implications for clinical practice', *Cancers*, 12(10), pp. 1–15. doi: 10.3390/cancers12102913.

Wang, F. *et al.* (2023) 'Metabolomic analysis - identi fi ed 2 - hydroxybutyric acid might be a key metabolite of severe preeclampsia'.

Wilson, W. H. *et al.* (2015) 'Targeting B cell receptor signaling with ibrutinib in diffuse large B cell lymphoma', 21(8), pp. 922–926. doi: 10.1038/nm.3884.Targeting.

Wilson, W. H. *et al.* (2021) 'Article Effect of ibrutinib with R-CHOP chemotherapy in genetic subtypes of DLBCL Graphical abstract Article Effect of ibrutinib with R-CHOP chemotherapy in genetic subtypes of DLBCL', *Cancer Cell*, pp. 1–11. doi: 10.1016/j.ccell.2021.10.006.

Wright, G. W. *et al.* (2020a) 'Article A Probabilistic Classification Tool for Genetic Subtypes of Diffuse Large B Cell Lymphoma with A Probabilistic Classification Tool for Genetic Subtypes of Diffuse Large B Cell Lymphoma with Therapeutic Implications', *Cancer Cell*, 37(4), pp. 551-568.e14. doi: 10.1016/j.ccell.2020.03.015.

Wright, G. W. *et al.* (2020b) 'Article A Probabilistic Classification Tool for Genetic Subtypes of Diffuse Large B Cell Lymphoma with A Probabilistic Classification Tool for Genetic Subtypes of Diffuse Large B Cell Lymphoma with Therapeutic Implications', *Cancer Cell*, 37(4), pp. 551-568.e14. doi: 10.1016/j.ccell.2020.03.015.

Xu-monette, Z. Y. *et al.* (2012) 'Mutational profile and prognostic significance of TP53 in diffuse large B-cell lymphoma patients treated with R-CHOP : report from an International DLBCL Rituximab-CHOP Consortium Program Study', 120(19), pp. 3986–3996. doi: 10.1182/blood-2012-05-433334.There.

Young, K. H. *et al.* (2007) 'Mutations in the DNA-binding codons of TP53 , which are associated with decreased expression of TRAIL receptor-2 , predict for poor survival in diffuse large B-cell lymphoma', 110(13), pp. 4396–4405. doi: 10.1182/blood-2007-02-072082.The.